Phases of Solid Methanol

Óscar Gálvez,* Belén Maté, Beatriz Martín-Llorente, Víctor J. Herrero, and Rafael Escribano

Instituto de Estructura de la Materia, CSIC, Serrano 123, 28006 Madrid, Spain

Received: November 21, 2008; Revised Manuscript Received: February 12, 2009

The solid phases of methanol were investigated using IR spectroscopy and numerical calculations with the SIESTA method. Improved spectra are reported of amorphous methanol at 90 K, and in particular of the α and β phases at 130 and 165 K, respectively, with assignments of bands not previously measured. The main features of the spectra of each phase are discussed and compared. A study of spectral changes with temperature leads to the conclusion that the metastable phase previously reported might be a mixture of the two known stable phases. Such a mixture could explain all spectral features observed in this investigation. The theoretical calculations provide reasonable agreement with the experimental data for most of the parameters, but predict H-bondings stronger than those observed. Differences between the spectra of the α and β phases are predicted with similar characteristics to the experimental results.

1. Introduction

The physicochemical properties of the liquid phase of methanol have been extensively studied, because of the relevance of methanol as a solvent and in many other applications. However, the solid state of methanol has not received that much attention. Solid methanol is a subject of interest in astrophysics, as it is a common component of interstellar icy grain mantles, with an average abundance of 17% with respect to water, the most abundant species (e.g., Williams et al.[1]). It is also present in our solar system, forming part of the ices on the surface of comets (e.g., Bockélee-Morvan[2]) and in several icy objects in the Kuiper belt (see, e.g., refs 3 and 4). In our planet, methanol can be found in the partially oxidized volatile organic compounds (POVOCs) that are involved in chemical reactions on atmospheric ice particles and aerosols.[5]

Solid methanol presents two stable crystalline phases that have been known for a long time, with a phase transition around 160 K.[6] The α phase is stable at lower temperatures, and the β phase is stable above 160 K until liquefaction, at ca. 175 K. Both crystals have orthorhombic symmetry and have been characterized by X-ray and neutron diffraction.[7−9] An amorphous phase of methanol is obtained by vapor deposition at low temperatures, transforming to the α phase upon warming at 130 K.[10,11] In addition, a metastable phase was recently proposed in the literature.[9,12] Torrie et al.[9] discovered this phase by quenching the β phase to low temperatures, although it was not obtained in every cycle of rapid cooling. This new phase was associated with the presence of a number of extra peaks in the diffraction pattern, in addition to those characteristic of the α phase. Further evidence was based on differences in the Raman spectra with respect to that of the α phase.[9] Later, Lucas et al.[12] claimed to obtain a metastable phase by vapor deposition at 130 K, that was stable upon warming to 145 K. They presented a mid-infrared spectrum for this phase showing some minor differences from their α phase spectrum.

In three early articles by Falk and Whalley,[10] Dempster and Zerbi,[11] and Pellegrini et al.,[13] an interpretation of the IR spectra of the α and β phases was put forward. The proposed assignment was facilitated using different deuterated samples, and a mathematical method of treating lattice dynamics was applied to assess this assignment.[11,13] In the first two works, minor differences between the IR spectra of the two crystalline phases (α and β) were found in the spectral region studied (between 300 and 4000 cm^{-1}). Dempster and Zerbi[11] mentioned that the only noticeable difference was a triplet observed at 1158, 1146, and 1142 cm^{-1} in the low-temperature phase that coalesced into a broader single peak with a maximum at 1040 cm^{-1} in the high-temperature phase. In the more recent spectra of Lucas et al.,[12] which included a spectrum assigned to the metastable phase, the differences were more evident (see Figure 3 in that paper), but they were not discussed.

We started this investigation with the purpose of providing new and complementary spectroscopic data on the phases of solid methanol. For the present contribution, solid methanol films were generated by vapor deposition from the gas phase on a noninteracting substrate, at different temperatures and pressures, in order to obtain all of the amorphous and crystalline phases. Special attention has been paid to the interpretation of relevant spectral differences between the phases. In addition, we have carried out a density functional theory (DFT) calculation of the structure of crystals of the α and β phases and a prediction of the corresponding infrared spectra. To the best of our knowledge, this is the first calculation of the crystal structures of methanol. Comparisons of the theoretical and experimental spectra are also presented.

2. Experimental Section

The experimental setup was described in detail before,[14,15] and only a brief description is provided here. Solid samples of CH_3OH were deposited from the vapor phase on a cold substrate located in a high-vacuum cylindrical chamber, evacuated by a turbomolecular pump. The temperature of the substrate was controlled, with ca. 1 K accuracy, between 80 and 250 K by means of a liquid nitrogen Dewar for cooling and a power transistor (2N3055) for heating. The background pressure in the chamber was usually around 10^{-7} mbar. The chamber was coupled to a Bruker Vertex70 Fourier transform infrared (FTIR) spectrometer through a purged pathway, with KBr windows for the incident and transmitted radiation, which focused on exiting

* To whom correspondence should be addressed. E-mail: ogalvez@iem.cfmac.csic.es.

10.1021/jp810239r CCC: $40.75
Published on Web 03/18/2009

onto a liquid-N_2-refrigerated mercury cadmium telluride (MCT) detector. In the transmission configuration used in this work, a 1-mm-thick Si wafer, at normal incidence with respect to the incoming infrared radiation, was used as the substrate. Spectra were recorded with a nominal resolution of 2 cm^{-1} (corresponding to ca. 0.5-cm mirror displacement in the interferometer), with co-addition of 300 scans for each spectrum. A quadrupole mass spectrometer (QMS) was used to check the purity of the sample during deposition. The absolute pressure in the deposition chamber was determined from the growth rate of the solid films on the substrate.[16] The film thickness values, needed for the calculation of the growth rate, were derived by simulating our transmission spectra with optical constants given by Hudgins et al.[17] for methanol ice at 75 K. A sticking coefficient of 1 and a density of 1.013 g/cm^3 were assumed at 80 K. The methanol density was derived from the 209.73 $Å^3$ unit cell volume given by Torrie et al.[9] for the α phase.

The calibration of the QMS remained stable over the course of the present experiments as verified by periodic checks. The estimated error in the absolute pressure values is ∼10%. In this work, we tested deposition pressures between 1×10^{-6} and 5×10^{-4} mbar. The maximum pressure value was limited by the operation regime of the turbomolecular pump. Finally, a pressure of 5×10^{-5} mbar and a temperature of 90 K were selected for film deposition.

Amorphous methanol films were generated by direct deposition at ∼90 K. Crystalline samples were prepared through a slow annealing (ca. 0.3 K/s) of the amorphous solid, heated to 130 K to form the α phase and to 165 K to produce the β phase. Above 145 K, solid methanol has a high sublimation rate in high vacuum, and to avoid sample losses, a controlled methanol pressure was maintained in the chamber. This pressure was adjusted at each temperature to avoid condensation or evaporation during the heating process. Attempts to generate the crystalline phases through direct deposition at higher temperatures were unsuccessful, most probably because of the low deposition pressures compatible with our experimental setup.

The background pressure of 10^{-7} mbar was mostly due to water molecules desorbing from the chamber walls, that co-deposited with methanol and could thus contaminate the solid methanol samples. Under our experimental conditions, with comparatively high deposition pressures (5×10^{-5} mbar) and short deposition times (40 s), the proportion of co-deposited water molecules contaminating the sample was estimated[16] to be ∼0.5%. Background water molecules could also be deposited during the measurements. The longest experiments, which included the annealing of the ice layer and the subsequent cooling to 90 K, lasted for about 10 min. During this time, the proportion of water molecules deposited would represent ∼5% of the methanol molecules in the ice layer. Most of these water molecules probably did not enter the sample, but rather formed a thin layer of ∼6 nm on top of the ∼300-nm methanol film. The IR spectra of the methanol ices should not be much affected by this small water contamination, and in fact, we did not observe appreciable changes over time in the methanol bands of static samples. In recent IR spectroscopic studies on ammonia-containing ices,[18,19] it has been pointed out that small amounts of water (∼1%) or other impurities can lead to changes of a few degrees in the phase transition temperature. Throughout the present work, we do not attempt to determine accurate phase transition temperatures from our IR spectra, and we believe therefore that the results discussed are not affected by the small contamination of the samples by background water molecules.

3. Calculations

We performed density functional theory (DFT) calculations with the SIESTA suite of programs,[20,21] using the Perdew−Burke−Ernzerhof[22] and Becke−Lee−Yang−Parr[23] exchange-correlation functionals of the generalized gradient approximation (GGA). The core electrons were substituted by norm-conserving pseudopotentials of Troullier Martins flavor, and the basis set for the valence electrons was a linear combination of atomic orbitals (LCAO) at double-Z polarized (DZP) level, localized within a soft confining potential[24] whose parameters were variationally obtained.[25] We selected a cutoff of 400 Ry for the real-space grid and 6 Å for the *k*-point sampling. The force tolerance parameter was set to 10^{-3} eV/Å, and the stress tolerance was set to 0.01 GPa.

Although both PBE and BLYP functionals predict an orthorhombic geometry of the unit cell and the same general arrangement of the molecules inside the cell, the results obtained with PBE highly overestimate the strength of hydrogen bonds between methanol molecules. This particularity of the PBE functional has also been found by our group in similar studies.[26] For this reason, we selected BLYP to compute the IR spectra of both phases, and only the BLYP results are included in the tabulated data.

The prediction of absorption intensities involves the calculation of the Born effective charges, proportional to the variation of the macroscopic polarization of the crystal with atomic displacements.[27] They were evaluated by numerical derivation of the macroscopic polarization, employing a step of 0.04 Bohr, the same value as in the force-constant calculations. The electronic contribution to the polarization was calculated using the Berry phase formalism,[28] by a discrete integration over the points of a grid, which we fixed in the present case as $25 \times 5 \times 5$, a value that induced a well-converged spectrum. Born charges need only be calculated for the atoms in the irreducible unit of the crystal, from which the appropriate values for the rest of atoms in the unit cell can be deduced by symmetry considerations.

Attempts to model the crystal structures of methanol were previously made by other authors,[29] using the VASP program,[30] but the crystal could not be optimized. A semiempirical calculation[13] using CNDO and treating the methanol molecules as members of polymer chains reproduced the crystal structure of the α phase and allowed for very good predictions of the spectra, as discussed below. Using the SIESTA method, a rapid convergence of the structures of the methanol crystal was obtained, which indicates that SIESTA might be a powerful tool for modeling these structures.

4. Results and Discussion

Experimental Part. Figure 1 presents a study of the low-temperature phases of solid methanol. Transmission IR spectra are shown of methanol deposited at 90 K (bottom trace, a), of the same sample after it had been warmed to 130 K (middle trace, b) and after subsequent cooling to 90 K (top, c). Vapor deposition at low temperature (<120 K) results in an amorphous phase, which presents a spectrum (a) similar to those recorded by Falk and Whalley,[10] Hudgins et al.,[17] and Bennett et al.[31] Table 1 summarizes the observed wavenumbers for the amorphous methanol bands recorded in this work and by other groups, including some bands that had not been recorded before, with the corresponding assignment, which, in some cases, might be uncertain. The overall agreement among previous and present investigations is acceptable.

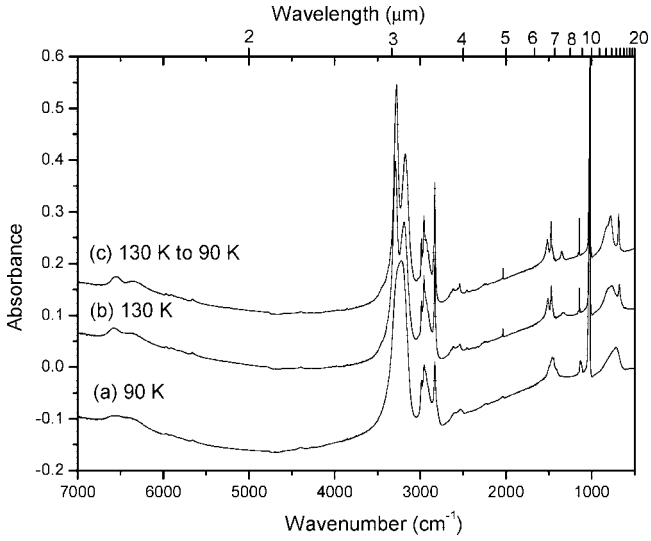

Figure 1. Infrared spectra of the low-temperature phases of methanol: (a) amorphous phase at 90 K, (b) α phase at 130 K obtained by warming the amorphous sample, and (c) α phase after the sample had been cooled again to 90 K. Spectra b and c are offset for clarity.

TABLE 1: Experimental Wavenumbers (cm^{-1}) and Assignment of the Amorphous Phase of Solid Methanol

assignment	90 K[a]	93 K[b]	75 K[c]	11 K[d]
ν_{12}	717	730	719	713, 834
ν_8	1026	1032	1029	1031, 1041
ν_7	1132, 1158	1114	1132	1113, 1120, 1128, 1137, 1157
ν_6	1415			1428
ν_5	1444			1444
ν_{10}	1461	1450	1460	1461
ν_4	1477			1478
?	1497			1495
$2\nu_8$	2039	2040	2036	2040
$2\nu_7$	2230			2237
?	2529	2537	2530	2527
?	2590	2607	2600	2601
ν_3	2831	2828	2831	2828
ν_9	2956	2951	2953	2961
ν_2	2985	2982	2982	2987
ν_1	3219	3235	3216	3080, 3187, 3274, 3389, 3426
?	4272			4270
?	4396			4402
$2\nu_3$	5658			
$2\nu_9$	5896			
$2\nu_2$	5972			
$2\nu_1$	6450			

[a] This work. [b] Falk and Whalley.[10] [c] Hudgins et al.[17] [d] Bennett et al.[31]

After the sample had been warmed to 130 K, the spectrum showed appreciable differences (Figure 1b) with respect to the cold trace. Sharper bands and multiple peaks appear in some regions (e.g., those of the ν_8, ν_7, and ν_1 normal modes). These modifications indicate the formation of the α crystalline phase, as observed in refs 10 and 11. Cooling the sample again to 90 K causes a slight blue shift and a sharpening of some bands (Figure 1c). These changes are completely reversible, and the spectrum transforms again to spectrum b when heated to 130 K, as mentioned previously for the temperature behavior of the α phase.[10] Table 2 presents a summary of the assignment of the spectra (the β phase is also included in this table; see below), from this work and from other groups. Our new observations in the high-frequency region are also listed in the table. The main particularities of the spectrum of the α phase, as mentioned in the literature and seen in our trace, are a narrow peak at ~680 cm^{-1}, a band structure around 1150 cm^{-1}, a resolved peak at ~1340 cm^{-1}, and a resolved double peak in the 3100−3300 cm^{-1} region. Inspection of the α phase spectrum of Falk and Whalley[10] (Figure 1 of that work) reveals all of these characteristics, despite the compressed scale of the paper publication. They can also be observed, except for the double peak in 3200−3300 cm^{-1} region due to saturation problems, in the spectrum of the α phase given by Dempster and Zerbi[11] in their Figure 1.

The spectra of Lucas et al.[12] require some discussion. These authors formed their methanol samples by direct vapor deposition on a silicon substrate at different temperatures. When they deposited methanol at 130 K they reported the presence of a crystalline phase that was stable until 145 K, where it transformed to the α phase. The phase between 130 and 145 K was called metastable, because the authors could not reproduce the corresponding spectrum by lowering the temperature from the α phase (see Figure 3 of Lucas et al.[12]). Although the quality of the spectra, recorded at 4 cm^{-1} resolution, is good, the figure is so compressed that it is difficult to ascertain in it the presence of some of the characteristic features mentioned above for the spectrum of the α phase, such as the band structure at 1150 cm^{-1}. The only appreciable differences between the two spectra are the double peak between 3200 and 3300 cm^{-1}, which is less resolved and has a different intensity pattern in the α phase, and the structure at 2900 cm^{-1}, which also seems less resolved in the α phase, but overall both spectra of ref 12 resemble that of our α phase displayed in Figure 1. The authors did not discuss the spectra in the text, referring to a forthcoming paper that, as far as we know, might not have been published later. The existence of a metastable phase will be further discussed below.

We present in the bottom trace a of Figure 2 the spectrum of the β phase of methanol. Noticeable changes in the spectra accompany the transformation from the α to the β phase. The spectral differences between these phases are better appreciated in the enlarged regions collected in Figure 3, where the lower trace corresponds to the α phase, recorded at 130 K, and the upper trace corresponds to the β phase, recorded at 165 K. Panel a represents the zone assigned to the ν_{12} normal mode. Bands at 677 and ~770 cm^{-1} in the α phase are merged into a broader band centered at 703 cm^{-1} in the spectrum of the β phase, as expected according to the symmetry of the unit cell.[10] Similarly, in the ν_7 region shown in panel b, the bands at 1145 and 1160 cm^{-1} in the α phase coalesce into a broader band at ca. 1147 cm^{-1} for the β phase. The bands ascribed to the ν_1 normal mode, located at 3176 and 3278 cm^{-1} in the low-temperature solid, are blue-shifted by 27 cm^{-1} in the high-temperature phase, and a similar behavior, with larger shifts of 42 and 60 cm^{-1}, respectively, is found for the first overtone ($2\nu_1$) components (panels c and d, respectively, of Figure 3). All of these frequency changes, with proposed assignments for the overtone region, which had not been analyzed before, are collected in Table 2. Falk and Whalley[10] commented that the differences between their spectrum of the high-temperature species at 165 K and that of the low-temperature phase were just broadenings of the bands due to temperature effects. As in our spectra, the main changes that they observed included a broadening in the ν_7 region and frequency shifts, although of smaller magnitude than ours, in the ν_1 region. Interestingly, their high-temperature spectrum had some contribution of the 680 cm^{-1} band that we observed to disappear in our spectra of the β phase. This could suggest that the high-temperature spectrum of ref 10 corresponds not to a pure β phase, but to a mixture with some minor

TABLE 2: Experimental Wavenumbers (cm^{-1}) for Different Methanol Crystal Structures

assignment	α phase[a]	β phase[a]	α phase[b]	α phase[c]	β phase[b]
ν_{12}	677, 764	703	685, 790	677, 770	675, 765
ν_8 (^{13}C)	1001, 1008	1003, 1011	1011		
ν_8	1020, 1025, 1032	1024, 1030, 1042	1029, 1046	1025	1030
ν_7 (^{13}C)	1114	1109		1114	
ν_7	1142, 1158	1133, 1147	1142, 1162	1143	1142
?	1334	1294	1345	1339	1300, 1370
ν_6?	1430		1426		1420
ν_5?	1456	1445	1445		
ν_{10}?	1472	1464	1458, 1470	1472	1459
?	1512	1515	1514	1512	
$2\nu_8$	2037	2043	2040	2036	2040
$2\nu_7$	2230, 2251, 2274	2227, 2252, 2274		2239	
?	2457	2453	2457	2458	2455
?	2537	2529	2538, 2562	2540	2540
?	2615	2614	2617	2615	2613
ν_3	2832	2832	2829	2835	2831
?	2907, 2929		2912		
ν_9	2958	2947	2955	2956	2954
ν_2	2985	2979	2982	2985	2980
ν_1	3189, 3291	3203, 3305	3187, 3284, 3443	3188, 3292	3193, 3297
?	3450	3450			
?	4272	4272			
?	4396	4396			
$2\nu_3$	5662	5662			
$2\nu_9$	5908	5895			
$2\nu_2$	5973	5951			
$2\nu_1$	6374, 6581	6382, 6608			

[a] This work, α phase at 130 K and β phase at 165 K. [b] Falk and Whalley,[10] α phase at 93 K and β phase at 165 K. [c] Hudgins et al.,[17] α phase at 120 K.

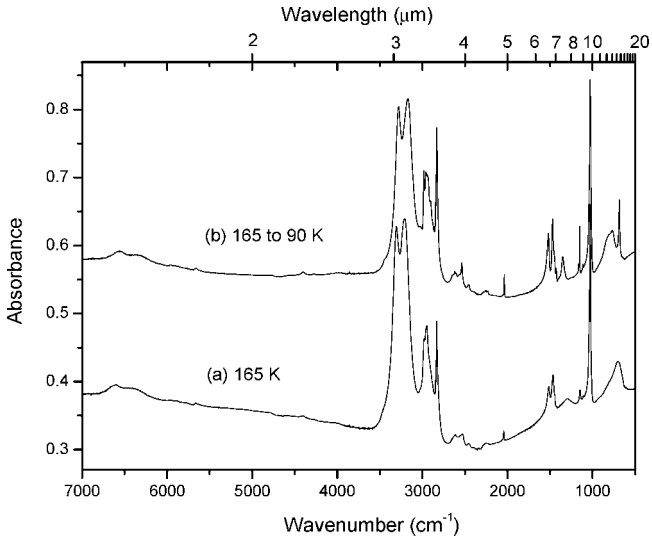

Figure 2. Infrared spectra of the high-temperature phase of solid methanol: (a) β phase at 165 K and (b) β phase after the sample had been cooled again to 90 K, offset for clarity.

participation of the α phase. This point will be discussed in detail in the Theoretical Part.

In an attempt to clarify the existence of a metastable phase, we followed the procedure described in the literature consisting of an abrupt cooling of the β phase to 90 K.[9] The IR spectrum thus obtained is represented as trace b in Figure 2. This spectrum shows some particularities: The ν_{12} region, around 700 cm^{-1}, looks similar to that of the α phase, whereas the ν_1 zone, around 3250 cm^{-1}, is like that of the high-temperature β phase. Other bands appear slightly shifted with respect to both the α and β phases. The β-to-α phase conversion is known to be a slow process, where kinetic effects play an important role.[32] In a different experiment, we cooled the β phase sample from 165 to 130 K and kept it at this temperature for an hour, monitoring any changes with the IR spectra. Special attention was paid to the $2\nu_8$ band, which appears at different frequencies in the two phases (see Table 2). Figure 4 provides a very interesting illustration of this process, showing both the displacement of this band in frequency and the preservation of the high-temperature component even after 55 min at 130 K. We interpret this result in terms of the slow transformation of the sample to a mixture of the β and α phases, with the degree of transformation depending on temperature and time. In all of the different experiments that we performed starting from the high-temperature phase, when a very rapid quenching or a slow cooling to 90 K was carried out, the low-temperature spectra presented features that can be ascribed to mixtures of the two phases. We conclude that, when the β phase is cooled, a mixture of the α and β phases is obtained, and only long periods of time at relatively high temperatures, on the order of 150 K, will probably allow a complete β-to-α phase transformation. Although we cannot completely discard the existence of a metastable phase, we can explain our experimental results by assuming the existence of just two crystalline phases, the α and β phases, that can coexist in some circumstances and in different proportions. This mixture could explain the differences in the IR and Raman spectra as well as neutron diffraction patterns, compared to the known features of each pure phase, which were taken as a confirmation of the possible existence of a metastable phase.[8,9,32] Nevertheless, further studies should be performed to clarify this point.

Theoretical Part. Using the SIESTA method with the parameters mentioned above, we have carried out an optimization of the structures of the α and β phases of the methanol crystal. A schematic picture of the converged structures is shown in Figure 5, and Table 3 gathers the most relevant parameters determined in this process, together with the experimental values where available.

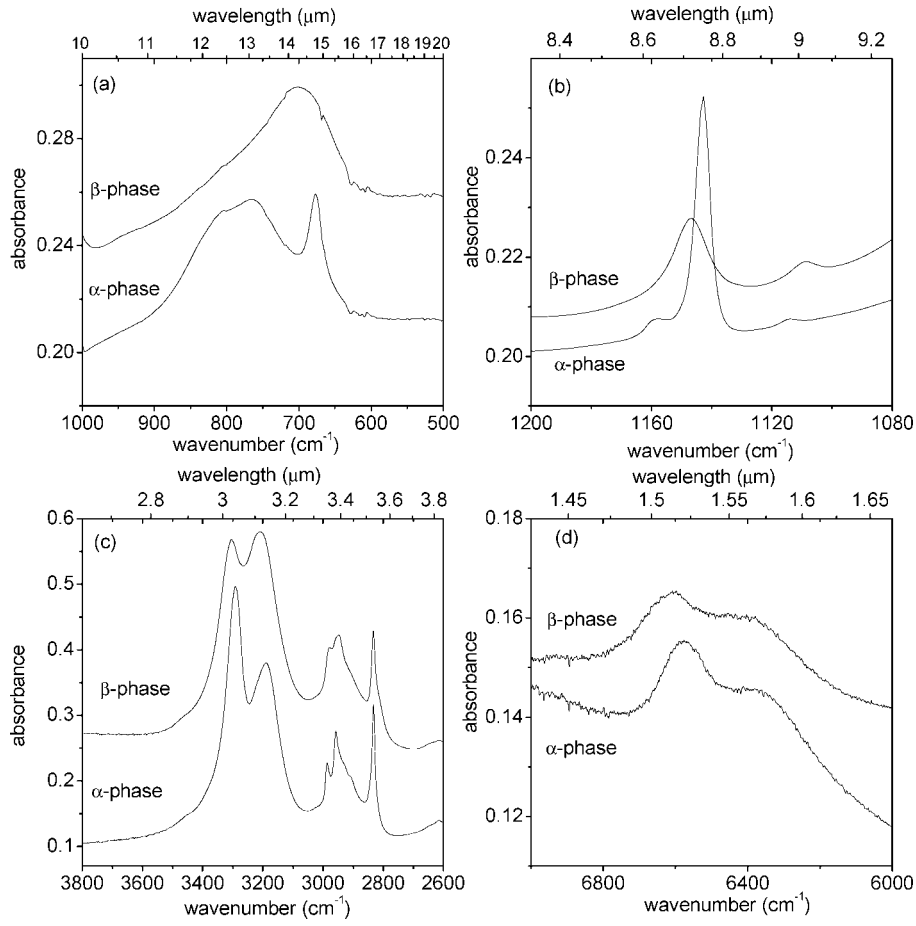

Figure 3. Detail of the most significant differences between the spectra of the α phase (130 K) and the β phase (165 K) of solid methanol, in the regions of (a) ν_{12}, (b) ν_7, (c) ν_1, and (d) $2\nu_1$. In all panels, the spectrum of the β phase has been offset for clarity.

As mentioned above, the calculations reflected the orthorhombic geometry of the unit cell for both phases, in agreement with the structural determination from X-ray diffraction measurements,[7] as well as that of Torrie et al. from neutron powder diffraction studies.[8,9] However, a clear disagreement exists in the prediction of the *a* lattice parameter of the α phase, which was overestimated ca. 20%. As can be observed in Figure 5, hydrogen bonds in this structure occur mainly in the *b*−*c* plane, whereas essentially dispersive forces between CH_3 groups are directed along the *a* axis. It is well-known that DFT methods do not properly reproduce dispersive forces, and in general, an expansion of the unit cell volume is expected in this kind of system, particularly along the axis on which these forces have a major contribution (see, e.g., ref 33), as happens in our systems.

In the early X-ray studies,[7] only the β phase could be unequivocally interpreted from the diffraction pattern, and the positions of the hydrogen atoms could not be solved. Torrie et al.[9] obtained the structural parameters of both phases by analyzing the neutron powder diffraction patterns of fully deuterated samples (CD_3OD). The structure of the α phase at 15 K had been previously measured by this group.[8] The geometrical parameters determined in that previous work were used to generate a rigid-body representation of the methanol molecule, which was then used in the analysis of the diffraction patterns of the α phase at 160 K and the β phase at 170 K. Only for the α phase could the rigid-body parameters be refined in the new analysis, unlike those of the β phase, because of the limited number of Bragg reflections obtained.[9] We have included in Table 3 the most relevant intra- and intermolecular parameters given in both works.[8,9] Significant differences appear in some of the values when these two works are compared, especially in the O—H1 distance and H2,3—C—H3,4 angles. In view of these discrepancies and the lack of refined experimental values for the β phase, the calculated results presented in this work acquire a special relevance, keeping in mind the approximations inherent to the theoretical method, especially those mentioned above.

The hydrogen bond formed in the solid induces a considerable elongation of the O—H1 distance compared to the value in the gas phase, as much as 0.06 Å in the 15 K structure of the α phase.[34,35] This effect is also reflected in the calculated H-bonding distances (O···H in Table 3), which are estimated ca. 0.04−0.08 Å shorter than those obtained by neutron powder diffraction, implying that the calculation predicted a greater transfer of the proton from its own methanol molecule to a nearby O atom of a neighboring molecule. Overall, for those parameters not involved in the H-bonding, our predicted intramolecular values are in better agreement with those measured at 15 K for the α phase, which is perhaps to be expected given that the calculated relaxation is assumed to model a zero-temperature condition. The calculated intermolecular parameters (O···O distance and C—O···O angle) are in reasonable agreement with those obtained in the X-ray diffraction experiments.[7]

From the Born charges calculated by the SIESTA method as mentioned in a previous section, the infrared spectrum can be predicted for the relaxed geometrical structures. Figure 6 and Table 4 collect our calculated infrared spectra for both phases of solid methanol. The figure reproduces the observed spectra

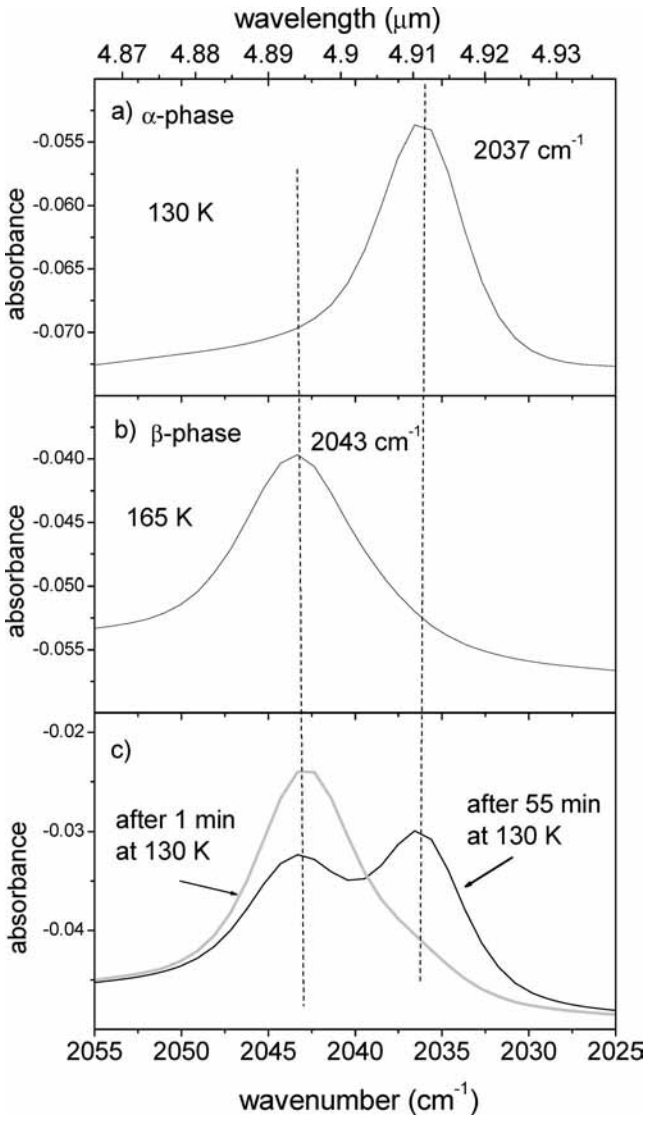

Figure 4. Infrared spectra of the $2\nu_8$ band of (a) the α phase at 130 K and (b) the β phase at 165 K and (c) evolution of the band when sample b was cooled to 130 K and kept at this temperature for 55 min.

at the top (panel a) and a bar diagram of the calculated wavenumbers and intensities at the bottom (panel c). In addition, to facilitate the comparison, we have included in panel b a representation of the predicted spectrum in which the calculated transitions are displayed as Lorentzian functions with a half-width at half-maximum (hwhm) of 40 cm^{-1} for the modes involving O—H stretching and bending and of 8 cm^{-1} for the rest of the bands. A discussion of the calculated results can be carried out with this information at hand. In general, the calculated and experimental frequencies are in reasonable agreement, deviating by less than 10% in most cases, which can be considered moderately satisfactory taking into account the uncertainties in the structural parameters for many of the atoms, especially the H, and the limitations of the calculations. Some of the predicted strongest bands in the low-frequency region, assigned to the C—O stretching normal mode, are close to those measured, deviating by less than 8%, and a similar result is obtained in the analysis of the CH_3 rocking band. A good agreement is found also for all three CH_3 stretching modes, in the high-frequency region of the spectrum.

However, it is in the O—H stretching modes where the major discrepancies emerge, the calculated values being red-shifted by up to ca. 250 cm^{-1}. These bands are predicted to have the highest intensity in the spectra, and the strong red shift found in the calculation is probably due to the large overestimation of the effect of the H-bonding, already made manifest in the previous discussion on bond distances, which weakens and elongates the corresponding intramolecular O—H bond.

Differences between the spectra of the α and β phase are found in the calculated results, in parallel to the experimental data. The strongest band of the C—O normal mode is predicted at slightly higher frequencies in the β phase, in agreement with the experimental spectra. A similar blue shift in the β phase with respect to the α phase is found for the CH_3 rocking band, observed in the experimental spectra too. The calculated O—H stretchings also appear at higher frequencies in the β phase than in the α phase, similarly to the observed spectra, although in this case the shift is much smaller. It is interesting to highlight the case of the O—H out-of-plane (oop) torsion band. Our experimental spectra show that only one band appears for this normal mode in the β phase structure, but two appear in the case of α phase (see Figure 3). The same result is predicted by our calculations. In the β phase structure, only one of the four bands assigned to the O—H oop normal mode has non-null intensity, whereas the opposite occurs for the α phase, according to the space-group analyses.[10] This result again suggests that previously recorded spectra of the β phase that show a double band in this region could, in fact, be mixtures of the two phases.

Pellegrini et al.[13] carried out a thorough investigation of this problem from a different point of view, by combining CNDO quantum calculations with an intra- and intermolecular force-constant refinement, which allowed them to reach a remarkable agreement between observed and calculated spectra. The method was also applied to study the variation of the spectra with the H-bonding angle linking pairs of molecules. This leads to the detection of a very large frequency dependence of the O—H and O···H torsional modes with this angle, which could explain the large width observed for the corresponding band. Some of the conclusions of that investigation specifically suggest that the structure seen by X-ray for the β phase could be an average of two distorted structures, very much in agreement with the line defended in the present work.

Relevant differences between the calculated spectra of the two phases appear in the lattice modes. However, there is not much information in the literature about this low-frequency region that we could use to compare with the calculations.

5. Summary and Conclusions

We present in this investigation a study of the different phases of solid methanol using infrared spectroscopy and supported by theoretical calculations. We have recorded spectra of the amorphous and crystalline phases of methanol, formed by vapor deposition on a cold substrate, in the range of temperature between 90 and 165 K. The spectra are assigned in agreement with previous works, and a tentative assignment is proposed for new bands in the high-frequency region of the spectra, between 4000 and 7000 cm^{-1}, not observed before. The higher quality and resolution of the spectra reveal in detail the structural variations that take place at the phase changes from the amorphous phase to the low-temperature α phase at 130 K and from this phase to the high-temperature β phase at 165 K. The former of these processes does not present any particular problems: the α phase, once it has been formed, is quite stable and reproducible in cooling and warming processes. Cooling the sample from 130 to 90 K induces a narrowing of the infrared bands in agreement with expectations.

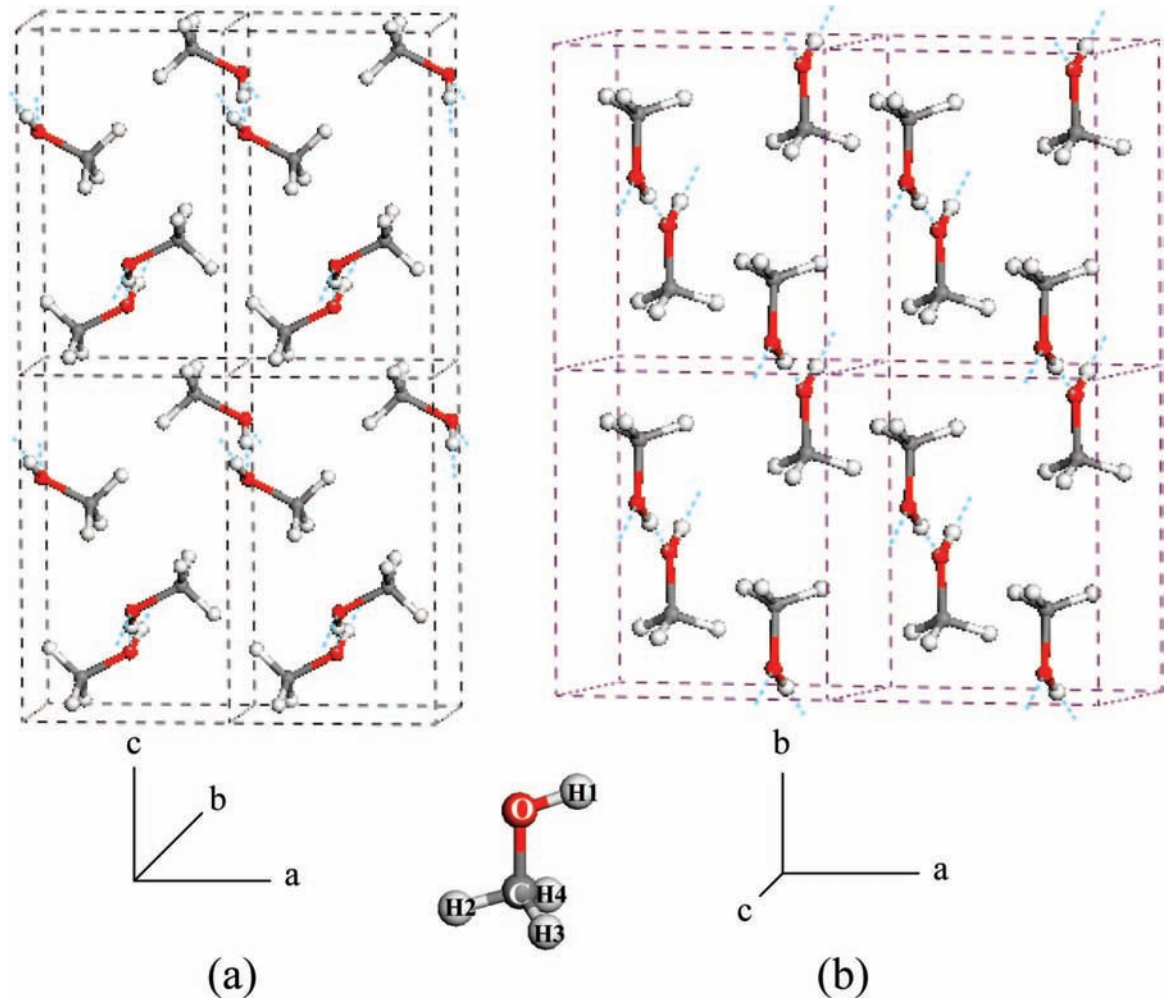

Figure 5. Calculated structure of methanol crystals: (a) α phase, (b) β phase. The dashed lines show the unit cell.

TABLE 3: Calculated (this work) and Experimental Lattice Parameters (Å), Bond Distances (Å), and Bond Angles (in degrees)

			experimental				
	calculated		α phase			β phase	
parameter	α phase	β phase	160 K[a]	15 K[b]	113 K[c]	170 K[a]	163 K[c]
a	6.057	6.690	4.9434	4.8728		6.04090	6.43 ± 0.02
b	4.526	7.506	4.6547	4.6411		7.1993	7.24 ± 0.02
c	8.842	4.740	9.1148	8.8671		4.6490	4.67 ± 0.02
V (Å^3)	242.4	238.0	209.73	200.53		214.51	217.40 ± 0.08
C—O	1.457	1.451	1.410	1.407	1.44	1.410[d]	1.42 ± 0.03
O—H1	1.017	1.010	0.960	1.011		0.960[d]	
C—H2	1.094	1.094	1.079	1.090		1.079[d]	
C—H3	1.098	1.097	1.084	1.059		1.084[d]	
C—H4	1.097	1.097	1.068	1.069		1.068[d]	
C—O—H1	109.5	110.6	106.5	110.2		106.5[d]	
H2—C—H3	108.8	108.9	100.9	108.4		100.9[d]	
H2—C—H4	109.3	108.9	115.2	106.7		115.2[d]	
H3—C—H4	109.4	109.7	108.7	113.5		108.7[d]	
O···H	1.665	1.664	1.710	1.744			
O···O	2.682	2.675	2.663	2.751	2.68		2.66 ± 0.03
C—O···O	109.4	124.4	109.7	118.2	108		119 ± 2

[a] Torrie et al.[9] [b] Torrie et al.[8] [c] Tauer and Lipscomb.[7] [d] Fixed to the rigid-body values of the α phase, column a.

The direct transition from the α to the β phase is a fast process at 165 K. However, the reciprocal transition is very slow and is not completed after 1 h of cooling at 130 K. Focusing on one particular band of the spectrum clearly shows the presence of a mixture of the two phases in this experiment. A metastable phase that was reported in the literature after sudden cooling of the β phase could in fact possibly consist in a mixture of the two stable phases, with different composition depending on the particular experimental conditions of the process. Such a mixture could account for all of the details found in our spectra.

The theoretical calculations were carried out using the SIESTA method, which has proved to be very reliable for this type of system. In the present case, there is a large uncertainty in some of the geometrical parameters determined experimen-

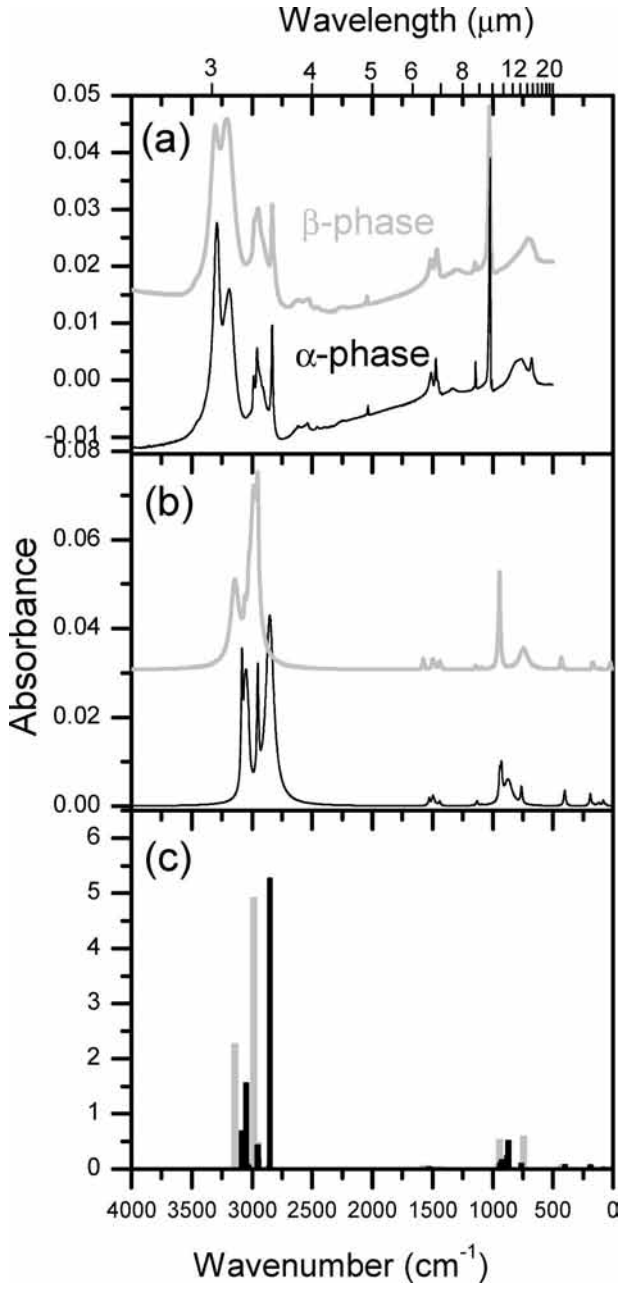

Figure 6. Comparison of (a) experimental and (b,c) calculated IR spectra of both phases of solid methanol. Bands in b are represented by Lorentzian curves with a hwhm of 40 cm^{-1} for H-bond-involved vibrations and 8 cm^{-1} for the rest of the bands. In c, stick spectra are displayed. In all panels, the spectrum of the β phase has been offset for clarity.

tally for both stable phases of methanol. The calculations reproduce reasonably well the structural data of the solids, but the H atoms involved in H-bonding are predicted at longer O—H intramolecular distances than observed; i.e., the H-bonds formed between neighbor molecules are stronger in the calculations than in the observed crystals. Accordingly, the calculated vibrational properties of the solids agree in good approximation with the observations, except for the vibrational modes that involve the stretching of the intramolecular O—H bonds, which are predicted at much lower frequencies than those measured experimentally.

The comparison of the spectra of the α and β phases shows similar characteristics both in the observed and in the calculated results. As a valuable result, our calculated spectra of the β phase show a single band for the OH oop normal mode, according to our experimental spectra and the space-group analysis of this crystal structure.

TABLE 4: Groups of Frequencies of Non-negligible Calculated Intensities of Solid Methanol with Appropriate Assignments, Compared to Experimentally Observed Transitions

	calculated		measured (this work)	
assignment	α phase	β phase	α phase	β phase
latt mode	83	24		
	190	169		
	401	430		
	408			
OH oop	762	744	677, 764	703
OH oop + CO str	870−879			
CO str	927−944	943−956	1025	1030
CH_3 rock	1130	1143	1142	1147
CH_3 bend, OH bend	1440−1527	1438−1577	1430−1472	1445−1464
CH_3 str sym	2950−2958	2952−2958	2832	2832
CH_3 str asym A″	3027−3029	3025−3028	2958	2947
CH_3 str asym A′	3062−3083	3058−3059	2985	2979
OH str	2852, 3046	2984, 3143	3189, 3291	3203, 3305

Acknowledgment. This research was carried out with funding from the Spanish Ministry of Education, Project FIS2007-61686. Ó.G. acknowledges financial support from the CSIC, "JAE-Doc" program. B. M.-Ll. acknowledges a studentship from Comunidad de Madrid and Fondo Social Europeo.

References and Notes

(1) Williams, D. A.; Brown, W. A.; Price, S. D.; Rawlings, J. M. C.; Viti, S. *Astron. Geophys.* **2007**, *48* (1), 25.
(2) Bockélee-Morvan, D. In *Molecules in Astrophysics: Probes and Processes*; van Dishoeck, E. F., Ed.; IAU Symposium 178; Kluwer Academic Publishers: Dordrecht, The Netherlands, 1997; p 222.
(3) Cruikshank, D. P.; Roush, T. L.; Bartholomew, M. J.; Geballe, T. R.; Pendleton, Y. J.; White, S. M.; Bell, J. F.; Davies, J. K.; Owen, T. C.; de Bergh, C.; Tholen, D. J.; Bernstein, M. P.; Brown, R. H.; Tryka, K. A.; Dalle Ore, C. M. *Icarus* **1998**, *135*, 389.
(4) Barucci, M. A.; Merlin, F.; Dotto, E.; Doressoundiram, A.; de Bergh, C. *Astron. Astrophys.* **2006**, *455*, 725.
(5) Abbatt, J. P. D. *Chem. Rev.* **2003**, *103*, 4783.
(6) Parks, G. S. *J. Am. Chem. Soc.* **1925**, *47*, 338.
(7) Tauer, K. J.; Lipscomb, W. N. *Acta Crystallogr.* **1952**, *5*, 606.
(8) Torrie, B. H.; Weng, S.-X.; Powell, B. M. *Mol. Phys.* **1989**, *67*, 575.
(9) Torrie, B. H.; Binbrek, O. S.; Strauss, M.; Swainson, I. P. *J. Solid State Chem.* **2002**, *166*, 415.
(10) Falk, M.; Whalley, E. *J. Chem. Phys.* **1961**, *34*, 1554.
(11) Dempster, A. N.; Zerbi, G. *J. Chem. Phys.* **1971**, *54*, 3600.
(12) Lucas, S.; Ferry, D.; Demirdjian, B.; Suzanne, J. *J. Phys. Chem. B* **2005**, *109*, 18103.
(13) Pellegrini, A.; Ferro, D. R.; Zerbi, G. *Mol. Phys.* **1973**, *26* (3), 577.
(14) Carrasco, E.; Castillo, J. M.; Escribano, R.; Herrero, V. J.; Moreno, M. A.; Rodríguez, J. *Rev. Sci. Instrum.* **2002**, *73*, 3469.
(15) Gálvez, O.; Maté, B.; Herrero, V. J.; Escribano, R. *Icarus* **2008**, *197*, 599.
(16) Maté, B.; Medialdea, A.; Moreno, M. A.; Escribano, R.; Herrero, V. J. *J. Phys. Chem. B* **2003**, *107* (40), 11098.
(17) Hudgins, D. M.; Sandford, S. A.; Allamandola, L. J.; Tielens, G. G. M. *Astrophys. J. Suppl. Ser.* **1993**, *86*, 713.
(18) Zheng, W.; Kaiser, R. I. *Chem. Phys. Lett.* **2007**, *440*, 229.
(19) Zheng, W.; Jewitt, D.; Osamura, Y.; Kaiser, R. I. *Astrophys. J.* **2008**, *647*, 1242.
(20) Ordejón, P.; Artacho, E.; Soler, J. M. *Phys. Rev. B* **1996**, *53*, 10441.
(21) Soler, J, M.; Artacho, E.; Gale, J. D.; García, A.; Junquera, J.; Ordejón, P.; Sánchez-Portal, D. *J. Phys.: Condens. Matter* **2002**, *14*, 2745.
(22) Perdew, J. P.; Burke, K.; Ernzerhof, M. *Phys. Rev. Lett.* **1996**, *77*, 3865.
(23) (a) Becke, A. D. *Phys. Rev. A.* **1988**, *38*, 3098. (b) Lee, C.; Yang, W.; Parr, R. G. *Phys. Rev. B* **1988**, *37*, 785.
(24) Junquera, J.; Paz, Ó.; Sánchez-Portal, D.; Artacho, E. *Phys. Rev. B* **2001**, *64*, 235111.
(25) Fernández Serra, M. V., Department of Physics and Astronomy, Stony Brook University, State University of New York. *Personal communication*, 2008. Parameters kindly provided by Fernández Serra.

(26) Fernández, D.; Botella, V.; Herrero, V. J.; Escribano, R. *J. Phys. Chem. B* **2003**, *107* (38), 10608.
(27) Fernández-Torre, D.; Escribano, R.; Archer, A.; Pruneda, J. M.; Artacho, A. *J. Phys. Chem. A* **2004**, *108*, 10535.
(28) King-Smith, R. D.; Vanderbilt, D. *Phys. Rev. B* **1993**, *47*, 1561.
(29) Natkaniec, I.; Holderna-Natkaniec, K.; Majerz, I.; Parlinski, K. *Chem. Phys.* **2005**, *317*, 171.
(30) (a) Kresse, G.; Furthmüller, J. *VASP*; Universität Wien: Vienna, Austria, 1999. (b) Kresse, G. *Phys. Rev. B* **1996**, *54*, 169. (c) Kresse, G. *Comput. Mater. Sci.* **1996**, *6*, 15.
(31) Bennett, C. J.; Chen, S.-J.; Sun, B.-J.; Chang, A. H. H.; Kaiser, R. I. *Astrophys. J.* **2007**, *660*, 1588.
(32) Anderson, A.; Andrews, B.; Meiering, E. M.; Torrie, B. H. *J. Raman Spectrosc.* **1988**, *19*, 85.
(33) Walker, M.; Pulham, C. R.; Morrison, C. A.; Allan, D. R.; Marshall, W. G. *Phys. Rev. B* **2006**, *73*, 224110.
(34) Lees, R. M. *J. Chem. Phys.* **1972**, *56*, 5887.
(35) Lees, R. M.; Baker, J. G. *J. Chem. Phys.* **1968**, *48*, 5299.

JP810239R